



Contents lists available at ScienceDirect

Biochemical and Biophysical Research Communications

journal homepage: [www.elsevier.com/locate/ybbrc](http://www.elsevier.com/locate/ybbrc)

## Cycloastragenol, a triterpene aglycone derived from *Radix astragali*, suppresses the accumulation of cytoplasmic lipid droplet in 3T3-L1 adipocytes



Shifeng Wang<sup>a</sup>, Chenxi Zhai<sup>a</sup>, Qing Liu<sup>a</sup>, Xing Wang<sup>a</sup>, Zhenzhen Ren<sup>a</sup>, Yuxin Zhang<sup>a</sup>, Yanling Zhang<sup>a</sup>, Qinghua Wu<sup>b</sup>, Shengnan Sun<sup>b</sup>, Shiyou Li<sup>c,\*</sup>, Yanjiang Qiao<sup>a,\*</sup>

<sup>a</sup>School of Chinese Pharmacy, Beijing University of Chinese Medicine, Beijing, China

<sup>b</sup>HD Biosciences Co., Ltd., Shanghai, China

<sup>c</sup>Beijing Institute of Genomics, Chinese Academy of Sciences, Beijing, China

### ARTICLE INFO

#### Article history:

Received 20 May 2014

Available online 2 June 2014

#### Keywords:

Cycloastragenol

*Radix astragali*

Adipogenesis

3T3-L1 adipocyte

Calcium mobilization

### ABSTRACT

Cycloastragenol (CAG), a bioactive triterpenoid sapogenin isolated from the Chinese herbal medicine *Radix astragali*, was reported to promote the phosphorylation of extracellular signal-regulated protein kinase (ERK). Here we investigated the effect of CAG on adipogenesis. The image-based Nile red staining analyses revealed that CAG dose dependently reduced cytoplasmic lipid droplet in 3T3-L1 adipocytes with the IC<sub>50</sub> value of 13.0 μM. Meanwhile, cytotoxicity assay provided evidence that CAG was free of injury on HepG2 cells up to 60 μM. In addition, using calcium mobilization assay, we observed that CAG stimulated calcium influx in 3T3-L1 preadipocytes with a dose dependent trend, the EC<sub>50</sub> value was determined as 21.9 μM. There were proofs that elevated intracellular calcium played a vital role in suppressing adipocyte differentiation. The current findings demonstrated that CAG was a potential therapeutic candidate for alleviating obesity and hyperlipidemia.

© 2014 Elsevier Inc. All rights reserved.

## 1. Introduction

Adipose tissue is a vital organelle for energy storage. Imbalance of energy intake and expenditure can easily contribute to cardio-metabolic disorders. Excess accumulation of cholesterol esters in arteries is intimately related to atherosclerosis, which can further develop into myocardial infarction, stroke or sudden cardiac death [1]. Now

**Abbreviations:** RA, *Radix astragali*; CAG, cycloastragenol; AG-IV, astragaloside IV; ERK, extracellular signal-regulated protein kinase; PFA, paraformaldehyde; Lova, Lovastatin; GSH, reduced glutathione level; ROS, reactive oxygen species; MMP, mitochondrial membrane potential; [Ca<sup>2+</sup>]<sub>i</sub>, intracellular calcium; 2APB, 2-aminoethoxydiphenyl borate; IBMX, 3-isobutyl-1-methylxanthine; TRP, transient receptor potential; TRPV1, transient receptor potential V1; TRPV2, transient receptor potential V2; TRPA1, transient receptor potential Ankyrin 1; IC<sub>50</sub>, 50% inhibitory concentration.

\* Corresponding authors. Address: Laboratory of Genome Variations and Precision Biomedicine, Beijing Institute of Genomics, Chinese Academy of Sciences, No. 1 Beichen West Road, Chaoyang District, Beijing, China. Fax: +86 10 8409 7628 (S. Li). Address: Key Laboratory of TCM-information Engineer of State Administration of TCM, School of Chinese Pharmacy, Beijing University of Chinese Medicine, No. 6 Wangjing Zhong Huan South Road, Chaoyang District, Beijing, China. Fax: +86 10 8473 8661 (Y. Qiao).

E-mail addresses: [lishiyou@big.ac.cn](mailto:lishiyou@big.ac.cn) (S. Li), [yjqiao@263.net](mailto:yjqiao@263.net) (Y. Qiao).

changes in human lifestyle and high-energy diet greatly increase the incidence of obesity [2–4], this risk factor even constitutes a threat to the population of children. There is an urgent need to develop safe ingredients to alleviate the diseases induced by fat accumulation. The traditional Chinese herbal medicine, however, supplies an abundance of natural compound resources for drug discovery.

3T3-L1 preadipocyte, originally derived from Swiss mouse embryo tissue, has served as an excellent in vitro model to discover active ingredients that are able to reduce the incidence of obesity [5]. When stimulated by hormone cocktail, transcription factors in adipocytes, such as peroxisome proliferator-activated receptor-γ (PPAR-γ) and CCAAT/enhancer binding protein (C/EBP), are activated, promoting adipogenesis [6]. Meanwhile, the adipocytes differentiation process might also be reversed by various conditions, such as modest hypoxia [7] and the intracellular calcium. Shi and Jensen et al. [8,9] revealed that the conversion of the preadipocyte into mature adipocyte was held back when the intracellular Ca<sup>2+</sup> level was elevated, by preventing postconfluency of preadipocytes, restricting c-myc expression and regulating cAMP level. The calcium ionophore A23187 and endoplasmic reticulum Ca<sup>2+</sup>-ATPase inhibitor thapsigargin were demonstrated to suppress adipogenesis through stimulating calcium influx [10].

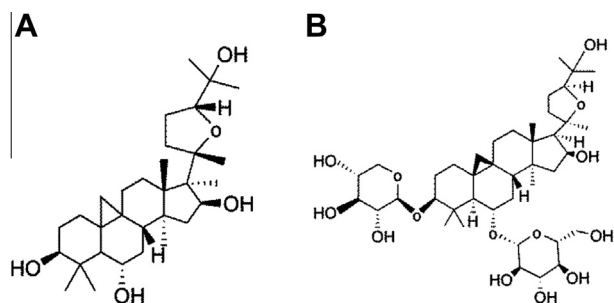


Fig. 1. Chemical structures (A) Cycloastragenol (CAG), (B) Astragaloside IV (AG-IV).

Cycloastragenol (CAG) (Fig. 1A), a cycloartane-type triterpene, derived from the Chinese herbal medicine *Radix astragali* (RA), was known for its ability to improve telomerase activity [11] and anti-aging [12]. RA was frequently prescribed by Chinese doctors in the therapy of hyperlipidemia, and was generally used in the form of crude extracts in Chinese formula Naoxintong [13]. Astragaloside IV (AG-IV) (Fig. 1B) [14] was another bioactive compound derived from RA that exhibited various bioactivities, such as anti-inflammation [15,16]. Recently, Yung et al. [17] reported that CAG and AG-IV stimulated extracellular signal-regulated protein kinase (ERK) phosphorylation in several cell types. We wondered whether CAG and AG-IV exerted any effects on adipocyte differentiation.

This study aimed to investigate the effects of CAG and AG-IV on inhibiting adipogenesis, in which we found that CAG suppressed lipid droplet accumulation in 3T3-L1 adipocytes. We also observed that CAG stimulated calcium mobilization in 3T3-L1 preadipocytes, suggesting a novel inhibitory mechanism of CAG on adipogenesis.

## 2. Materials and methods

### 2.1. Materials

Cycloastragenol and astragaloside IV were purchased from the National Institutes for Food and Drug Control (China), the purities exceeded 98%. The other chemicals used in the current experiments were obtained from Sigma Chemical Co (St Louis, MO, USA) if not stated otherwise. The chemicals were dissolved in DMSO to make stock solutions and were stored at  $-20^{\circ}\text{C}$ .

### 2.2. Cell culture

3T3-L1 preadipocyte and HepG2 cell lines were purchased from American Type Culture Collection (ATCC). The cells were cultured in Dulbecco's modified Eagles's medium (DMEM) containing 10% fetal bovine serum (Gibco, USA), 500 U/mL penicillin and 500  $\mu\text{g}/\text{mL}$  streptomycin at  $37^{\circ}\text{C}$ , 5%  $\text{CO}_2$ .

### 2.3. Differentiation of 3T3-L1 preadipocytes

For 3T3-L1 preadipocytes differentiation, the cells were plated in 96-well clear-bottom black plates (Corning, USA) at 3000 cells per well. The cells were cultured at humid atmosphere for 2 days, and were then treated with tested compound for 1 day. During the adipocytes differentiation procedure, the adipocytes were continuously incubated with tested compound for 7 days. The differentiation was carried out according to the protocol as described previously [18]. Briefly, the medium was changed to 0.5 mM 3-isobutyl-1-methylxanthine (IBMX), 0.25  $\mu\text{M}$  dexamethasone, 1  $\mu\text{g}/\text{mL}$  insulin and 2  $\mu\text{M}$  rosiglitazone for 2 days. Subsequently, the culture medium was replaced with DMEM containing 1  $\mu\text{g}/\text{mL}$  insulin for another 2 days. Thereafter, the cells were further cultured for 2 days with complete DMEM. Fresh compound was added during changing the culture medium.

### 2.4. Nile red staining and lipid droplet determination

Cytoplasmic lipid droplet in 3T3-L1 adipocytes was measured by Nile red staining on day 10 [19]. First, the cells were fixed with 4% paraformaldehyde (PFA) for 20 min at room temperature (RT). Second, the cells were stained with final 5  $\mu\text{g}/\text{mL}$  Nile red solution for 10 min. Third, the cells were stained with final 10  $\mu\text{g}/\text{mL}$  Hoechst 33342 solution for 15 min. The cells were rinsed three times with phosphate-buffered saline (PBS) after each manipulation. Fluorescence intensities of nuclear and lipid droplet were captured by Cellomics ArrayScanVTI reader (Thermo, USA) at 386 nm and 485 nm, respectively.

Percentage of lipid droplet in 3T3-L1 adipocytes was calculated as the following formula:  $100 \times \{\text{RFU}_{\text{sample}} - \text{RFU}_{\text{control(-)}}\} / \{\text{RFU}_{\text{control(+)}} - \text{RFU}_{\text{control(-)}}\}$ , where RFU means relative fluorescence unit; sample means compound treated mature adipocytes; control(-) means undifferentiated preadipocytes; control(+) means 0.25% DMSO treated mature adipocytes.

### 2.5. Cytotoxicity assay

Cytotoxicity evaluation of CAG was performed using ToxInsight Kit (Thermo, USA) according to the recommended instructions. Briefly, HepG2 cells were seeded in 96-well plate at the density of 8000 cells per well and incubated overnight. Then, the cells were treated with eight concentrations of tested chemical, which was 1:2 serially diluted. The final top concentrations of CAG, Lovastatin, aspirin and gemfibrozil were 60  $\mu\text{M}$ , 10  $\mu\text{M}$ , 553  $\mu\text{M}$  and 850  $\mu\text{M}$ , respectively. Each concentration was performed in triplicate. Vehicle control cells were treated with 0.25% DMSO. After 24 h, the culture medium was replaced with 100  $\mu\text{L}$  ToxInsight staining solution, the plate was incubated for 45 min at  $37^{\circ}\text{C}$ . Thereafter, the cells were rinsed once with 100  $\mu\text{L}$  Hank's Balanced Salt Solution (HBSS). The images of HepG2 cells were captured using Cellomics ArrayScanVTI reader immediately.

### 2.6. Intracellular calcium mobilization detection

The calcium influx in 3T3-L1 cells was performed according to the procedures described previously [20]. In brief, 3T3-L1 preadipocytes were seeded in 96-well black plates at the density of 20,000 cells per well and were cultured overnight. Prior to recordings, the cells were incubated for 30 min at  $37^{\circ}\text{C}$  in HBSS containing 4  $\mu\text{M}$  Fluo-4 (Molecular Devices, USA), 2.5 mM probenecid and 2 mM Acid Red 1 (Sigma, USA). The FlexStation II (Molecular Devices, USA) was employed to record the calcium signal, with 485 nm excitation and 525 nm emission wavelengths. The percentage of the intracellular calcium was calculated as the following formula:  $100 \times \{\text{RFU}_{\text{sample}} - \text{RFU}_{\text{control(-)}}\} / \{\text{RFU}_{\text{control(+)}} - \text{RFU}_{\text{control(-)}}\}$ , where RFU means relative fluorescence unit of calcium signal.

### 2.7. Statistical analysis

Data were presented as mean  $\pm$  SEM. Statistical significance of the differences was identified by unpaired Student's *t* - test or one-way ANOVA using GraphPad Prism 5.0.  $^*P < 0.05$  was defined as statistical significance.

## 3. Results and discussion

### 3.1. Effect of CAG on lipid droplet accumulation in 3T3-L1 adipocytes

To investigate the effects of CAG and AG-IV on adipogenesis of 3T3-L1 adipocytes, Lovastatin (Lova), an inhibitor of HMG-CoA reductase [21], was employed as the positive control. As shown

in Fig. 2A, the lipid droplet was remarkably induced in the cytoplasm of 3T3-L1 adipocytes and 10  $\mu\text{M}$  CAG exhibited prominent inhibitory effect. It reduced lipid content by nearly 35% compared with vehicle control treated adipocytes (Fig. 2B), while lipid droplets were not reduced in AG-IV treated adipocytes ( $P > 0.05$ ,  $n = 6$ ).

To further study the actions of CAG on lipid droplet accumulation in 3T3-L1 adipocytes, we investigated the effects of CAG at various concentrations. As shown in Fig. 2C, a dose response trend was observed, less cytoplasmic lipid droplet accumulated with increased concentration of CAG treatment. The  $\text{IC}_{50}$  value of CAG was determined as 13.0  $\mu\text{M}$ .

Adipocyte proliferation is a notable characteristic involved in cell differentiation [22]. Now findings suggest that adipogenesis comprises at least two stages, which are disparately linked to cell

growth [23]. In the current study, we observed that the 3T3-L1 cell number was increased by induction of differentiation, treated with 60  $\mu\text{M}$  CAG or 10  $\mu\text{M}$  Lova, the cell number of adipocytes profoundly declined compared with control condition ( $P < 0.001$ ), but again, there were no significant differences between undifferentiated preadipocytes and CAG treated cells (Fig. 2D). These findings indicated that when up to 60  $\mu\text{M}$ , CAG suppressed 3T3-L1 adipocytes differentiation as well as cell growth; while below 30  $\mu\text{M}$ , it merely inhibited lipid droplet accumulations in the cytoplasm but had no influence on cell growth.

In some cases, cell loss may occur to adipocytes when exposed to acute toxic substrates. Declined total fluorescence intensity of lipid droplet would then be detected. Consequently, chances of acquiring false positive responses might increase. In the current study, we measured the anti-adipogenic effect of CAG by normalizing lipid

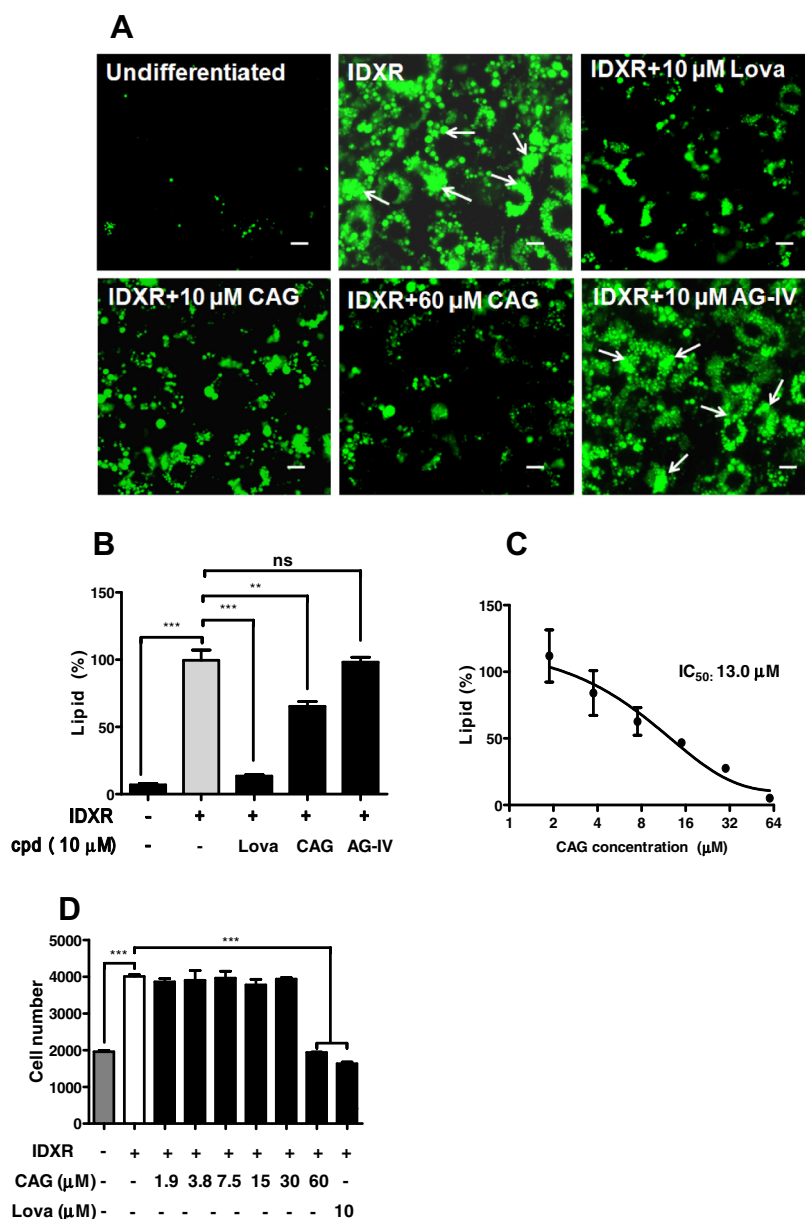


**Fig. 2.** CAG prevents adipogenesis of 3T3-L1 adipocytes (A) Differentiation of 3T3-L1 preadipocytes treated with or without tested compounds. The images were captured by 20 $\times$  magnification using Cellomics HCS ArrayScanVTI reader. Scale bars, 25  $\mu\text{m}$ . (B) Analysis of lipid droplet in average single adipocyte treated with CAG, AG-IV or Lova, respectively. Fluorescence intensity of Nile red staining is normalized to percentage of differentiated control adipocytes. (C) Dose response curve of CAG on lipid droplet accumulation in 3T3-L1 adipocytes. (D) Cell number of adipocytes after IDX differentiation and compound treatment for 7 days. Data shows mean  $\pm$  SEM of three independent experiments.  $n = 6$ .  $**P < 0.01$ ;  $***P < 0.001$ ; n.s., not significant.

droplet in average single adipocyte, which may avoid the false positive conditions caused by acute cytotoxicity.

### 3.2. CAG did not induce injury of HepG2 cells

Drug induced toxicity is a principal reason for drug nonapprovals and withdrawals [24]. As CAG or Lova treatment significantly reduced the cell number of differentiated 3T3-L1 adipocytes, we further conducted toxicity tests of CAG on HepG2 cells; the tested concentrations of CAG were in accordance with its effect on preventing the adipogenesis. Cell loss, reduced glutathione level (GSH), reactive oxygen species (ROS) and mitochondrial membrane potential (MMP) were assessed as toxicity markers [25,26]. Here aspirin worked as a non-toxic control and was used to determine the safety thresholds. Gemfibrozil, an anti-hyperlipidemia drug, was used as a positive control [27,28].

Fig. 3A shows that HepG2 cells treated with CAG and Lova are as integrated as the cells incubated with aspirin. The normalized dose responses of CAG were listed in Fig. 3B–E, the curves of CAG were within the thresholds and thus we flagged it as non-toxic. Consistent with our results, Nancy [29] reported that no obvious sub-chronic toxicity induced by CAG was observed. On the contrary, exposure of cells to gemfibrozil resulted in decline of cell number and glutathione depletion, ROS formation in the nuclear area, and MMP disruption. This finding further indicated that the reduced cell number of 3T3-L1 adipocytes by CAG was not induced by acute cytotoxicity, but due to the inhibitory effect on 3T3-L1 adipocyte-differentiation.

### 3.3. CAG stimulated calcium mobilization in 3T3-L1 preadipocytes

A variety of transient receptor potential (TRP) channels have been found endogenously expressed in 3T3-L1 preadipocytes

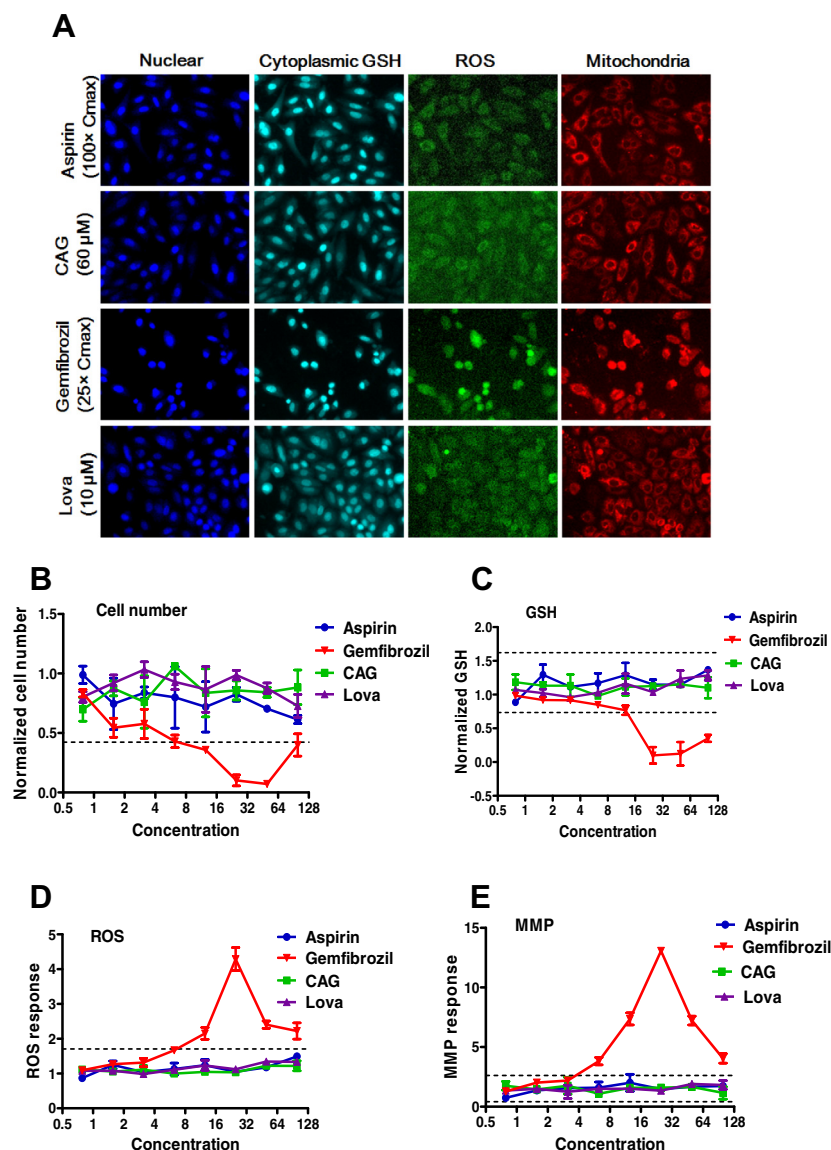


**Fig. 3.** CAG did not induce injury of HepG2 cells. HepG2 cells incubated with or without tested compounds for 24 h were probed with specific fluorescent dyes to detect cellular targets. Cell images were captured by 10 $\times$  magnification using the Cellomics ArrayScan VTI reader. (A) Representative images of nuclear, reduced glutathione level (GSH), reactive oxygen species (ROS) and mitochondrial membrane potential (MMP) in HepG2 cells treated with tested compounds. (B) Normalized response plot of cell number. (C) Normalized response plot of cellular GSH, GSH level was determined by the total cytoplasmic fluorescence intensity. (D) Normalized response plot of ROS formation, ROS was quantified by the total intensity in the nuclear area. (E) Normalized response plot of MMP, MMP means the difference of average fluorescence intensity between nuclear and cytoplasm. Broken lines in the dose response plot were thresholds, they were determined by mean normalized response of aspirin  $\pm 3 \times$  SD, if any of the targets' response goes beyond the toxicity thresholds, the tested compound is flagged as toxic.



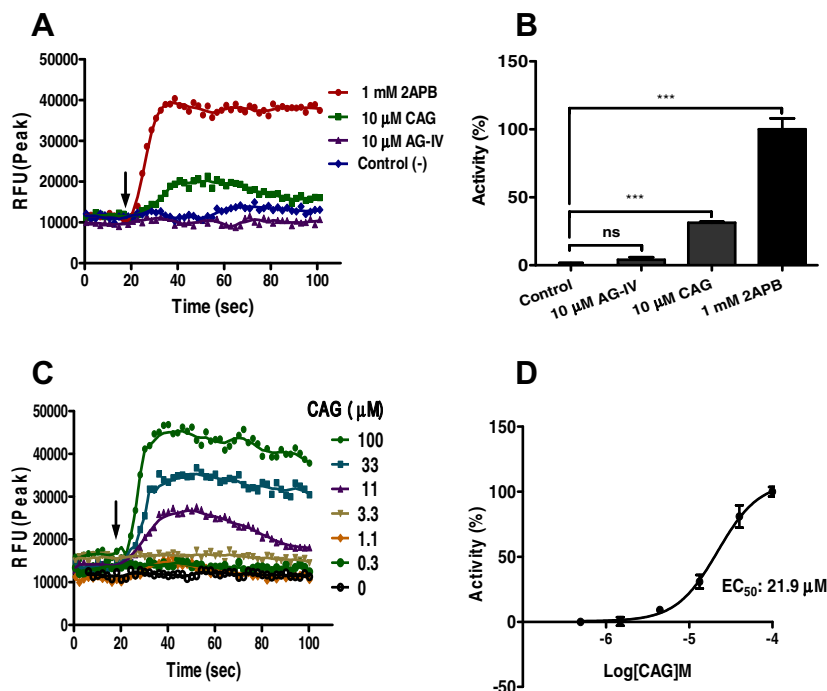


**Fig. 4.** CAG induced calcium mobilization in 3T3-L1 preadipocytes. 3T3-L1 preadipocytes were loaded with Fluo-4 and the calcium signal was captured with FlexStation II. (A) Representative profiles illustrating the time-course of the increased calcium evoked by application of 10  $\mu\text{M}$  tested compounds. The arrow indicated the onset of compound application; (B) Analysis of the calcium level in 3T3-L1 preadipocytes treated with or without compounds; (C) Representative responses of the increased calcium level in 3T3-L1 preadipocytes after infusion of CAG; (D) Dose response curve of CAG on calcium mobilization. Activity means normalized intracellular calcium level. The percentage of calcium signal was calculated as the following formula:  $100 \times \frac{\text{RFU}_{\text{sample}} - \text{RFU}_{\text{control(-)}}}{\text{RFU}_{\text{control(+)}} - \text{RFU}_{\text{control(-)}}$ .  $n = 6$  for each group, data were mean  $\pm$  SEM, \*\*\* $P < 0.001$ , n.s., not significant.

[30], and some of these ion channels were reported to regulate the process of lipid metabolism, such as transient receptor potential V1 (TRPV1) [31].

To investigate the target molecules of CAG, a panel of TRP channels was profiled using calcium influx assays on transfected HEK293 cells. We have developed a series of cell lines stably expressing TRP channels after nuclear transfection as reported previously [32], including TRPV1, and transient receptor potential V2 (TRPV2), transient receptor potential Ankyrin 1 (TRPA1). The results showed that CAG stimulated calcium influx in each transfected HEK293 cell line (data not shown). Since activation of TRP channels was closely related to calcium influx [33,34], we suspected that CAG might be able to non-selectively stimulate intracellular calcium mobilization.

Then, we tested the effect of CAG on calcium mobilization in 3T3-L1 preadipocytes, 2-aminoethoxydiphenyl borate (2APB) [35,36] was used as a positive control. The results showed that a significant increase of  $[\text{Ca}^{2+}]_i$  was provoked by perfusion of 3T3-L1 preadipocytes with 10  $\mu\text{M}$  CAG ( $P < 0.001$ ). In a parallel study, the intracellular calcium level was not modified by application of AG-IV (Fig. 4A and B). Further, we measured the dose response of CAG on calcium influx. Representative profiles illustrating the time-course of the calcium level evoked by administration of CAG are shown in Fig. 4C. CAG stimulated calcium mobilization in a dose dependent manner (Fig. 4D), the  $\text{EC}_{50}$  value was determined as 21.9  $\mu\text{M}$ .

In contrast to our results, Lisa et al. [17] reported that increased  $[\text{Ca}^{2+}]_i$  was not observed by treatment of HEK293 cells with CAG. This difference may be due to different tested concentrations of CAG. We stimulated 3T3-L1 preadipocytes and HEK293 cells with 10  $\mu\text{M}$  CAG, while the top concentration of CAG investigated by Lisa et al. was 100 nM.

Previous studies revealed that an elevated  $\text{Ca}^{2+}$  level was implicated in inhibiting adipocyte differentiation [8,37]. It is likely that

CAG stimulated  $[\text{Ca}^{2+}]_i$ , thereby restrained intracellular lipid droplet accumulation. In addition, the effect of CAG might be associated with its special structure of a triterpenoid sapogenin. AG-IV, however, was unable to induce calcium influx and possessed no remarkable effect on adipogenesis.

In conclusion, the present study demonstrated that CAG inhibited lipid droplet accumulation in 3T3-L1 adipocytes, which may offer a potential strategy for the treatment of obesity related diseases. We further discovered that CAG could increase  $[\text{Ca}^{2+}]_i$  in 3T3-L1 preadipocytes and may elicit favorable responses in preventing the adipogenesis.

#### Acknowledgments

This work was supported by grants of the National Key Technology R&D Program of China-Identification Technology of Active Clusters of Traditional Chinese Medicine (2008BAI51B01); and the National High Technology Research and Development Program of China (2011ZX09201-201-26), and the Key Laboratory for Traditional Chinese Medicine basic Research and New Drug Discovery (2013-SYSKFKT-04). The authors thank Profs. Youwen He for his valuable suggestions, and Dr. Ziyuan Liu for critical reading and editing the manuscript.

#### References

- [1] N. Kraemer, R.V. Farese Jr., T.C. Walther, Balancing the fat: lipid droplets and human disease, *EMBO Mol. Med.* 5 (2013) 905–915.
- [2] B. Klop, J.W. Elte, M.C. Cabezas, Dyslipidemia in obesity: mechanisms and potential targets, *Nutrients* 5 (2013) 1218–1240.
- [3] P.G. Kopelman, Obesity as a medical problem, *Nature* 404 (2000) 635–643.
- [4] K.E. Corey, L.M. Kaplan, Obesity and liver disease: the epidemic of the twenty-first century, *Clin. Liver Dis.* 18 (2014) 1–18.
- [5] M. Draganow, R. Cameron, P. Narayan, S. O'Carroll, Image-based high-throughput quantification of cellular fat accumulation, *J. Biomol. Screen.* 12 (2013) 999–1005.

- [6] F.M. Gregoire, C.M. Smas, H.S. Sul, Understanding adipocyte differentiation, *Physiol. Rev.* 78 (1998) 783–809.
- [7] T. Hashimoto, T. Yokokawa, Y. Endo, N. Iwanaka, K. Higashida, S. Taguchi, Modest hypoxia significantly reduces triglyceride content and lipid droplet size in 3T3-L1 adipocytes, *Biochem. Biophys. Res. Commun.* 440 (2013) 43–49.
- [8] H. Shi, Y.D. Halvorsen, P.N. Ellis, W.O. Wilkison, M.B. Zemel, Role of intracellular calcium in human adipocyte differentiation, *Physiol. Genomics* 3 (2000) 75–82.
- [9] B. Jensen, M.C. Farach-Carson, E. Kenaley, K.A. Akanbi, High extracellular calcium attenuates adipogenesis in 3T3-L1 preadipocytes, *Exp. Cell Res.* 301 (2004) 280–292.
- [10] T. Takova, J.M. Takova, Role of  $Ca^{2+}$  in the early stages of murine adipocyte differentiation as evidenced by calcium mobilizing agents, *Differentiation* 60 (1996) 151–158.
- [11] S.R. Fauce, B.D. Jamieson, A.C. Chin, R.T. Mitsuyasu, S.T. Parish, H.L. Ng, et al., Telomerase-based pharmacologic enhancement of antiviral function of human CD8+ T lymphocytes, *J. Immunol.* 181 (2008) 7400–7406.
- [12] T.M. Rickabaugh, B.D. Jamieson, A challenge for the future: aging and HIV infection, *Immunol. Res.* 48 (2010) 59–71.
- [13] J. Zhao, H. Zhu, S. Wang, X. Ma, X. Liu, C. Wang, et al., Naioxintong protects against atherosclerosis through lipid-lowering and inhibiting maturation of dendritic cells in LDL receptor knockout mice fed a high-fat diet, *Curr. Pharm. Des.* 19 (2013) 5891–5896.
- [14] J. Zhu, S. Lee, M.K. Ho, Y. Hu, H. Pang, F.C. Lp, et al., In vitro intestinal absorption and first-pass intestinal and hepatic metabolism of cycloastragenol, a potent small molecule telomerase activator, *Drug Metab. Pharmacokinet.* 25 (2010) 477–486.
- [15] J. Yang, H.X. Wang, Y.J. Zhang, Y.H. Yang, M.L. Lu, J. Zhang, et al., Astragaloside IV attenuates inflammatory cytokines by inhibiting TLR4/NF- $\kappa$ B signaling pathway in isoproterenol-induced myocardial hypertrophy, *J. Ethnopharmacol.* 150 (2013) 1062–1070.
- [16] D.Y. Lee, H.J. Noh, J. Choi, K.H. Lee, M.H. Lee, J.H. Lee, et al., Anti-inflammatory cycloartane-type saponins of *Astragalus membranaceus*, *Molecules* 18 (2013) 3725–3732.
- [17] L.Y. Yung, W.S. Lam, M.K. Ho, Y. Hu, F.C. Lp, H. Pang, et al., Astragaloside IV and cycloastragenol stimulate the phosphorylation of extracellular signal-regulated protein kinase in multiple cell types, *Planta Med.* 78 (2012) 115–121.
- [18] K. Zebisch, V. Voigt, M. Wabitsch, M. Brandsch, Protocol for effective differentiation of 3T3-L1 cells to adipocytes, *Anal. Biochem.* 425 (2012) 88–90.
- [19] P. Greenspan, E.P. Mayer, S.D. Fowler, Nile red: a selective fluorescent stain for intracellular lipid droplets, *J. Cell Biol.* 100 (1985) 965–973.
- [20] Q. Liu, J. Liu, H. Guo, S. Sun, S. Wang, Y. Zhang, et al., [6]-gingerol: a novel  $AT_1$  antagonist for the treatment of cardiovascular disease, *Planta Med.* 79 (2013) 322–326.
- [21] J.A. Tobert, Lovastatin and beyond: the history of the HMG-CoA reductase inhibitors, *Nat. Rev. Drug Discov.* 2 (2003) 517–526.
- [22] L. Mališová, Z. Kováčová, M. Koc, J. Kračmerová, V. Stich, L. Rossmeislová, Ursodeoxycholic acid but not tauroursodeoxycholic acid inhibits proliferation and differentiation of human subcutaneous adipocytes, *PLoS ONE* 8 (2013) 1–11.
- [23] W. Guo, K.M. Zhang, K. Tu, Y.X. Li, L. Zhu, H.S. Xiao, et al., Adipogenesis licensing and execution are disparately linked to cell proliferation, *Cell Res.* 19 (2009) 216–223.
- [24] L. Tolosa, S. Pinto, M.T. Donata, A. Lahoz, J.V. Castell, J.E. O'Connor, et al., Development of a multiparametric cell-based protocol to screen and classify the hepatotoxicity potential of drugs, *Toxicol. Sci.* 127 (2012) 187–198.
- [25] D. Wu, Al. Cederbaum, Removal of glutathione produces apoptosis and necrosis in HepG2 cells overexpressing CYP2E1, *Alcohol. Clin. Exp. Res.* 25 (2001) 619–628.
- [26] R. Heidari, H. Babaei, M.A. Eghbal, Cytoprotective effects of organosulfur compounds against methimazole induced toxicity in isolated rat hepatocytes, *Adv. Pharm. Bull.* 3 (2013) 135–141.
- [27] A. Liu, S. Xie, H. Sun, F.J. Gonzalez, X. Wei, R. Dai, Myotoxicity of gemfibrozil in cynomolgus monkey model and its relationship to pharmacokinetic properties, *Toxicol. Appl. Pharmacol.* 235 (2009) 287–295.
- [28] P. Domínguez Tordera, J.F. Comellas Alabern, J.F. Comellas Alabern, F. Ronda Rivero, Gemfibrozil hepatotoxicity: a case report, *Int. J. Clin. Pharm.* 33 (2011) 730–732.
- [29] N.J. Szabo, Dietary safety of cycloastragenol from *Astragalus* spp.: subchronic toxicity and genotoxicity studies, *Food Chem. Toxicol.* 64 (2014) 322–334.
- [30] M. Bishnoi, K.K. Kondepudi, A. Gupta, A. Karmase, R.K. Boparai, Expression of multiple transient receptor potential channel genes in murine 3T3-L1 cell lines and adipose tissue, *Pharmacol. Rep.* 65 (2013) 751–755.
- [31] L.L. Zhang, D. Yan Liu, L.Q. Ma, Z.D. Luo, T.B. Cao, et al., Activation of transient receptor potential vanilloid type-1 channel prevents adipogenesis and obesity, *Circ. Res.* 100 (2007) 1063–1070.
- [32] L.H. Ma, Y. Deng, B. Zhang, Y.Q. Bai, J. Cao, S.Y. Li, et al., Pinacidil, a  $K_{ATP}$  channel opener, identified as a novel agonist for TRPA1, *Chin. Sci. Bull.* 57 (2012) 1810–1817.
- [33] M. Gees, B. Colsooul, B. Nilius, The role of transient receptor potential cation channels in  $Ca^{2+}$  signaling, *Cold Spring Harb. Perspect Biol.* 2 (2010) 1–31.
- [34] B. Minke, TRP channels and  $Ca^{2+}$  signaling, *Cell Calcium* 40 (2006) 261–275.
- [35] K.H. Chen, X.H. Xu, Y. Liu, Y. Hu, M.W. Jin, G.R. Li, TRPM7 channels regulate proliferation and adipogenesis in 3T3-L1 preadipocytes, *J. Cell. Physiol.* 229 (2014) 60–67.
- [36] Ö. Kaplan, M. Nazıroğlu, M. Güney, M. Aykur, Non-steroidal anti-inflammatory drug modulates oxidative stress and calcium ion levels in the neutrophils of patients with primary dysmenorrhea, *J. Reprod. Immunol.* 100 (2013) 87–92.
- [37] E. Szabo, Y. Qiu, S. Baksh, M. Michalak, O. Michal, Calreticulin inhibits commitment to adipocyte differentiation, *J. Cell Biol.* 182 (2008) 103–116.